Science of the Total Environment 755 (2021) 142240

Contents lists available at ScienceDirect

Science of the Total Environment

journal homepage: www.elsevier.com/locate/scitotenv

Road salt retention and transport through vadose zone soils to shallow groundwater

Teresa Baraza *, Elizabeth A. Hasenmueller

Department of Earth and Atmospheric Sciences, Saint Louis University, Saint Louis, MO 63108, United States

HIGHLIGHTS

- Deicer retention in soil occurs via slow porewater flow and ion exchange reactions.
- Ion exchange with Na^+ from NaCl causes loss of soil base cations and nutrients.
- Retention in soil delays road salt delivery to groundwater by months.
- Karst conduit flow paths cause rapid release of salt ions to groundwater.
- Karst systems feature dual road salt delivery pathways to aquifers.

GRAPHICAL ABSTRACT

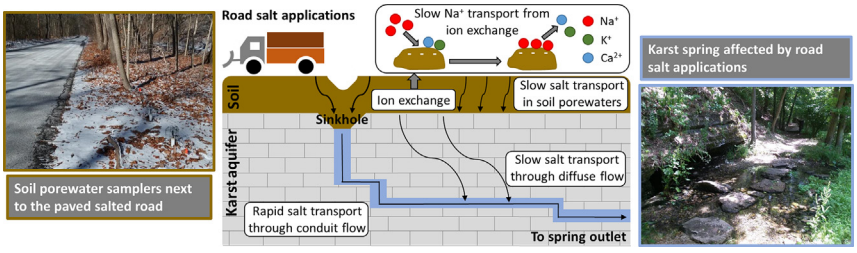

ARTICLE INFO

Article history:
Received 22 May 2020
Received in revised form 31 August 2020
Accepted 4 September 2020
Available online 15 September 2020

Editor: Jay Gan

Keywords:
Road salt
Cation exchange
Soil
Vadose zone
Karst
Groundwater
Urban geochemistry

ABSTRACT

Increasing background salinity in watersheds has largely been attributed to road salt retention in groundwaters due to their long residence times. However, laboratory studies demonstrate that soils temporarily store salts, either in porewater or adsorbed onto particles. Field studies of road salt retention in soils are nevertheless rare, and mechanisms of salt transport across multiple hydrological reservoirs (e.g., from soil to groundwater) are unknown. Thus, we collected roadside soil porewater and karst spring water weekly for ~1.5 yr to determine salt transport through the vadose zone into the phreatic zone. We observed dual retention mechanisms of sodium (Na^+) and chloride (Cl^-) in soils due to slow porewater movement, causing ion movement through the soil as slow as 1.3 cm/day, and cation exchange processes, leading to initial Na^+ retention followed by later release months after application. Cation exchange processes also caused base cation loss from exchange sites into mobile porewater. Rapid Na^+ and Cl^- delivery to groundwater occurred through karst conduits during the winter. However, elevated background levels of salt ions in groundwater during the non-salting months indicated accumulation in the catchment due to slower porewater flow in the soil and rock matrix and delayed Na^+ release from soil exchange sites.

1. Introduction

Road deicing salts are widely used during the winter because of their effectiveness in improving road safety, but their use can have unintended environmental consequences. Rapid salt dissolution causes the delivery of high concentrations of sodium (Na^+), chloride (Cl^-), and other contaminants into roadside environments (Corsi et al., 2010; Harte and Trowbridge, 2010; Moore et al., 2017; Thunqvist, 2004). Most of the freshwater contamination caused by deicing salts is localized near roads (especially in urbanized areas with dense networks of roadways) and is directly related to the amount of salt applied (Foos, 2003). Thus, impervious land cover has been demonstrated to be a good predictor of Cl^- contamination in surface waters (Dugan et al., 2017; Moore et al., 2020). High concentrations of road salts can drastically change the chemical signature of natural waters, causing

* Corresponding author.
E-mail address: teresa.barazapiazuelo@slu.edu (T. Baraza).

https://doi.org/10.1016/j.scitotenv.2020.142240
0048-9697/

calcium-magnesium-bicarbonate (Ca^{2+}-Mg^{2+}-HCO_3^-)-dominated waters to become Na^+-Cl^--dominated waters (Moore et al., 2017). These changes can have significant effects on freshwater aquatic organisms (Potapova and Charles, 2003), especially if deicing agent ions like Cl^- reach chronic (230 mg/L) or acute (860 mg/L) toxicity levels (Clements and Kotalik, 2016; Corsi et al., 2010, 2015; U.S. Environmental Protection Agency, 1988). Increased Cl^- concentrations in waters can also decrease drinking water quality and lead to corrosion of water distribution systems, vehicles, bridges, and other infrastructure (Bird et al., 2018; Stets et al., 2018).

Many studies have observed abnormally high and increasing Na^+ and Cl^- concentrations in surface waters (Bird et al., 2018; Corsi et al., 2015; Dugan et al., 2017; Godwin et al., 2003; Haake and Knouft, 2019; Kaushal et al., 2018; Kelly et al., 2008; Meriano et al., 2009; Moore et al., 2020; Novotny et al., 2008; Ostendorf et al., 2001; Scott et al., 2019) and groundwaters (Rhodes and Guswa, 2016; Robinson and Hasenmueller, 2017; Vitale et al., 2017). The observed persistence of road salts in surface waters and groundwaters over both short and long timeframes suggests retention of these ions within watersheds, either through conservative (e.g., slow water movement) or non-conservative mechanisms (e.g., ion exchange reactions, uptake by plants or microorganisms). Traditionally, Na^+ is considered to behave less conservatively than Cl^-. Indeed, Na^+:Cl^- ratios below 1 in streams and groundwater-fed springs suggest higher Na^+ retention within the system (Meriano et al., 2009; Moore et al., 2017; Robinson and Hasenmueller, 2017; Snodgrass et al., 2017).

In many hydrologic systems, water often passes through soil before it reaches surface waters and groundwaters. The main drivers of Na^+ retention are likely slow porewater movement and cation exchange on soil particles, whereby Na^+ is retained in the soil and other cations, such as Ca^{2+}, Mg^{2+}, and potassium (K^+), are mobilized into the soil solution (Meriano et al., 2009; Rhodes and Guswa, 2016; Rossi et al., 2017). Watershed Cl^- retention has also been observed. For example, mass balance studies for Cl^- in a watershed in Toronto, Canada, found that only about 45% of the road salt applied was discharged directly into streams, suggesting that the remaining Cl^- entered a temporary storage pool in the subsurface (Howard and Haynes, 1993; Perera et al., 2013). Mechanisms for Cl^- retention in watershed soils include conservative processes, like slow and/or heterogeneous flow paths, but also non-conservative processes, like anion exchange, uptake by vegetation and microbes, and chlorination of organic matter (OM) (Bastviken et al., 2007).

To test the interactions of road salts and soils, laboratory flushing experiments, where soil cores were irrigated with a brine solution (meant to mimic salt-rich runoff from roads due to deicing applications) followed by dilute water (meant to mimic runoff with low dissolved salt content that occurs during the non-salting period), demonstrated temporary retention of Na^+ and Cl^- in soils (Kincaid and Findlay, 2009; Robinson et al., 2017). Another study collected porewaters from a soil next to an interstate highway to investigate the interactions between the soil and deicing salts under field conditions (Rossi et al., 2017). They found that relatively high Na^+ and Cl^- concentrations persisted throughout the year, suggesting slow transport and temporary retention of these ions in the soil. Nevertheless, the interactions between deicing salts and soils near more common and smaller paved roads are still largely unknown.

In addition to Na^+ and Cl^- retention, road salts can also affect the soil's chemical and physical properties. Ion exchange processes can lead to the replacement and consequent leaching of base cations and plant nutrients, such as Ca^{2+}, Mg^{2+}, and K^+, when excessive amounts of Na^+ are introduced to the system (Rossi et al., 2017). This process can lead to soils becoming sodic, which has detrimental effects on plant growth (Asensio et al., 2017; Willmert et al., 2018). Excessive salt inputs to soils can also cause changes in soil pH, which can disrupt major geochemical fluxes such as the nitrogen (N) cycle (Green et al., 2008; Lancaster et al., 2016). Furthermore, laboratory studies have shown that road deicing salts cause the mobilization of toxic trace elements from soils by cation and anion exchange, Cl^- complex formation, and colloid dispersion due to high exchangeable Na^+ percentage (ESP) values (Amrhein et al., 1992; Fay and Shi, 2012; Nelson et al., 2009; Norrström and Jacks, 1998; Sun et al., 2015; Wu and Kim, 2017).

Because water commonly interacts with soil before it reaches surface waters and groundwaters, soils may constitute one of the main storage pools for salt ions in watersheds. Yet, the interactions between road deicing salts and the vadose zone remain unclear, particularly under field conditions. Furthermore, an integrated study of the timing of road salt movement through different hydrological reservoirs (e.g., from soil to groundwater) has not yet been performed. These interactions become even more complex in systems such as karst aquifers, which are characterized by dual porosity that causes both fast (e.g., conduit) and slow (e.g., diffuse matrix) flow paths. Thus, to understand the role of soils in the transport and retention of Na^+ and Cl^- after road salt applications, we collected in situ soil porewater and karst groundwater samples for ~1.5 yr. Soil water samples were collected at different distances from a paved and salted road as well as varying depths. The objectives of this study were to characterize: 1) Na^+ and Cl^- retention and movement through the vadose zone as a function of space and time, 2) the behavior of other major cations in soil water in relation to road salt applications to identify any ion exchange reactions and the timing of those exchanges, and 3) the transport and timing of Na^+ and Cl^- between hydrological reservoirs (i.e., from vadose zone soils to groundwaters).

2. Materials and methods

2.1. Study location

To investigate road salt movement through soil to the shallow groundwater, soil porewater and karst groundwater samples were collected at the Rockwoods Reservation (Wildwood, Missouri, United States; Fig. 1), which is managed by the Missouri Department of Conservation (MDC). The regional climate at the study site is temperate with respective long-term (1946 to 2019) temperature and precipitation averages of 13.6 °C and 97.5 cm/yr (NOAA, 2019). Average total snow accumulation, which is included as melt equivalent in the average annual precipitation value, is 47.9 cm/yr (NOAA, 2019). During the study period, average monthly precipitation was above the long-term average at 10.5 cm/month. Total snowfall during the winters of 2017–2018 and 2018–2019 had respective values of 18.0 cm and 61.5 cm. Winters are generally mild in the area, with air temperatures rarely remaining below 0 °C for longer than a few days (NOAA, 2019). Thus, snow typically starts melting within ~3 days of deposition (or earlier in the case of paved roads that have been salted), and a sustained snowpack is rare (Haake and Knouft, 2019). Atmospheric deposition of Na^+ and Cl^- in the region was <0.003 mM during the study period (NADP, 2020).

The Rockwoods Reservation features karst topography, with sinkholes, caves, losing streams, and several springs. We sampled the largest spring at the site, Rockwoods Spring, as a proxy for the shallow groundwater. Rockwoods Spring issues from an outcropping of the Middle Ordovician Plattin Group, a unit of gray mudstone interbedded with laminated grainstone (Harrison, 1997). Limestone comprises 95% of the total rock volume in the unit, but the bedrock also features minor amounts of shale, clay, and chert (Shourd and Levin, 1976). Soils overlay nearly all the bedrock at the study site. These soils belong to the Horsecreek silt loam unit in the Gasconade Rock outcrop complex (U.S. Department of Agriculture, 2020). The Horsecreek silt loam unit is a well-drained soil, leading to fast infiltration and low runoff. Soils are classified as nonsaline to very slightly saline (0.0–2.0 mmhos/cm; U.S. Department of Agriculture, 2020). Soil OM content ranges from 5 wt% to 19 wt% (Robinson et al., 2017).

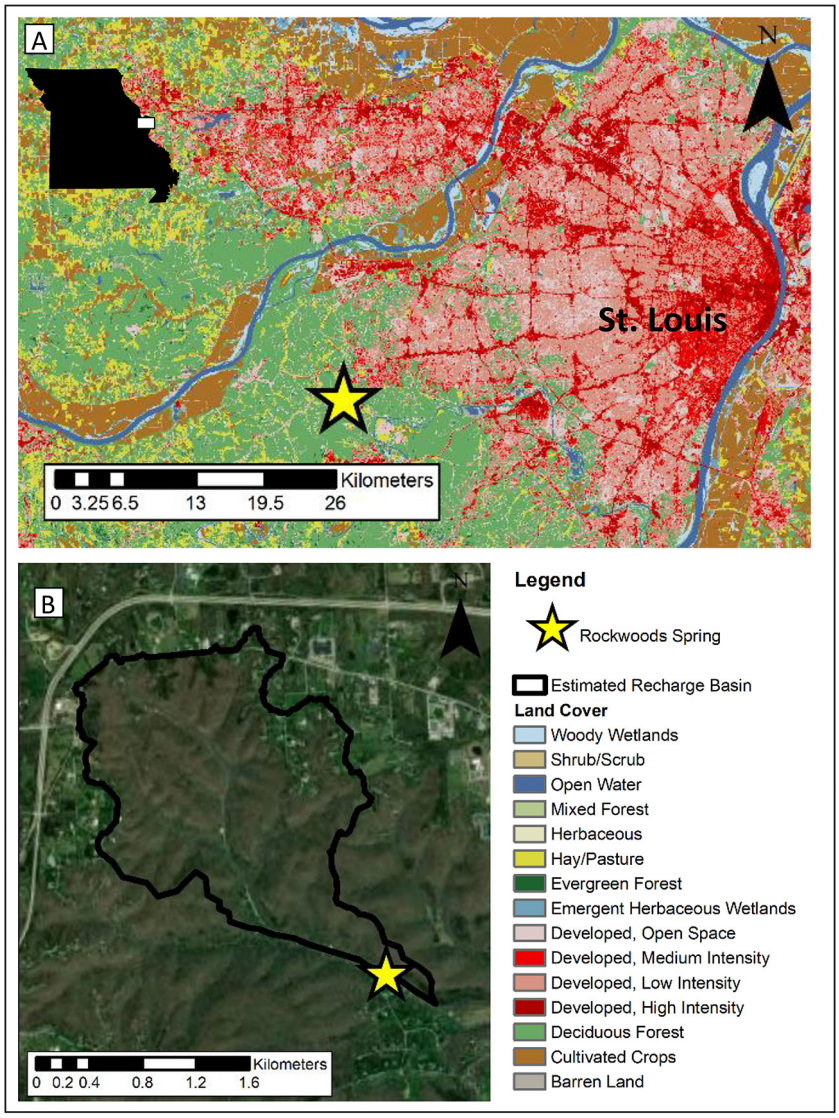

Fig. 1. A) Land cover map showing the location of Rockwoods Spring in Wildwood, Missouri, United States, southwest of the Saint Louis metropolitan area. B) Delineation of the estimated Rockwoods Spring recharge basin based on topography (data from Robinson and Hasenmueller, 2017).

Detailed studies focused on the isotope hydrology of Rockwoods Spring indicate a water retention time in the aquifer of ~1 yr, suggesting the aquifer is relatively shallow in the subsurface (Frederickson and Criss, 1999; Criss et al., 2007; Hasenmueller and Criss, 2013). The spring has a median discharge of 0.03 m^3/s and peak flows as high as 0.31 m^3/s (Robinson and Hasenmueller, 2017). Rockwood Spring's recharge area is estimated at ~3.6 km^2, with land use classified as 96% vegetative coverage, 3% impervious surface area (ISA; specifically, 1.4% roads, 0.8% additional paved surfaces like sidewalks and parking lots, and 0.8% other impervious surfaces), and 1% bare earth or open water (Robinson and Hasenmueller, 2017). In spite of the relatively low percentage of ISA within the spring's recharge area, road salt contamination has previously been detected at Rockwoods Spring (Hasenmueller, 2011; Hasenmueller and Criss, 2013; Robinson and Hasenmueller, 2017). Supplemental material Section 1.1 includes additional details about the site's hydrochemistry.

Soil porewaters were collected weekly from 25 February 2018 to 30 May 2019, and groundwater samples were collected weekly from 1 November 2017 to 31 July 2019. Road salting in the Rockwoods Reservation occurred across 0.025 km^2 (0.7% of the total recharge area) of paved surfaces within the park boundaries. The 2017–2018 salting period began on 16 January 2018 and finished on 21 February 2018, with three application events and a total of 6804 kg of salt applied. The 2018–2019 salting period started on 15 November 2018 and ended on 3 March 2019, with 12 application events and 12,637 kg of salt applied (Table S1). Thus, during the 2017–2018 and 2018–2019 road salting periods, total salt applications on paved surfaces within the park were 0.3 kg/m^2 and 0.6 kg/m^2, respectively. However, the estimated aquifer recharge area (Fig. 1; from Robinson and Hasenmueller, 2017) also encompasses paved areas outside of the park limits for which we do not have road salt application data. Consequently, the aquifer received higher inputs of road salts than those calculated for the Rockwoods Reservation alone. Estimations of the road salt applications performed outside of the Rockwoods Reservation are detailed in Supplemental material Section 1.2.

2.2. Soil porewater, groundwater, and road deicing salt sampling and analysis

Soil porewater samples were collected using 10 porous-cup suction lysimeters (i.e., the 1900 Soil Water Sampler; SoilMoisture Equipment Corp.) installed near a road at the Rockwood Reservation. The 10

lysimeters were distributed in four nests (A, B, C, and D) at different distances from the paved road (1.0 m, 1.5 m, 4.0 m, and 18.0 m, respectively), different depths (10 cm and 20 cm samplers at all the nests and additional 50 cm samplers at nests B and C where soils were deep enough), and different topographic slope angles (Fig. S1). Nests A, B, and C were located closest to the road in a relatively flat area. Thus, they were expected to receive salt inputs from deicing applications to the road. Nest D was located farthest from the road (18.0 m), and was thus unlikely to receive salt splash from the road. The nest was also on a steep, forested slope that drained towards the road, so nest D was not expected to receive salt inputs from drainage towards the site. Thus, nest D acted as a control for porewater chemistry. Details on the installation of the lysimeters and soil water collection are provided in Supplemental material Section 1.3. Grab samples from Rockwoods Spring were also collected approximately weekly to use as a proxy for shallow groundwater. Additionally, a sample of the road salt applied on paved surfaces in the study area was obtained for analysis.

All water samples and the diluted road salt sample were filtered through 0.2-μm filters into 50-mL polypropylene vials for elemental concentration analyses via ion chromatography (IC) and inductively coupled plasma optical emission spectrometry (ICP-OES). Samples were stored at 4 °C until analysis. A ThermoFisher Dionex Integrion HPIC IC was used for Cl^- analysis of samples. Instrument accuracy and precision were respectively ±6.1% and ±0.4%, based on check standards and sample duplicates. Subsamples for ICP-OES analysis were acidified to 1% HNO_3, then major cations (Na^+, Ca^{2+}, Mg^{2+}, K^+, and silicon (Si^{4+})) were measured with a PerkinElmer Optima 8300 ICP-OES. Instrument precision was ±3.5%.

Aliquots for oxygen (O) and hydrogen (H) isotope ratio analyses (i.e., $\delta^{18}O$ and δ^2H, respectively) were collected when soil porewater and spring sample volumes were >10 mL. Water isotope subsamples were filtered through 0.45-μm filters into 2-mL glass vials with no headspace and stored at room temperature until analysis. Values of $\delta^{18}O$ and δ^2H in water samples were obtained with a Picarro L2130-i cavity ring-down spectrometer. Instrument precision was ±0.04‰ for $\delta^{18}O$ and ± 0.23‰ for δ^2H. Results are reported as $\delta^{18}O$ and δ^2H relative to Vienna standard mean ocean water (V-SMOW).

In addition to chemical analyses of grab samples, in situ water quality and level data were collected for the spring. In detail, Cl^- concentrations were continuously monitored at 5-min intervals using a YSI 6600 V2 Multiparameter Water Quality Sonde; data were corrected for drift using the R package, driftR (Shaughnessy et al., 2019). Point measurements of Cl^- concentrations were also taken weekly using a YSI Professional Plus Multiparameter handheld instrument. Stage was continuously monitored (5-min intervals) in the spring using a Solinst Levelogger Edge pressure transducer. Data from the water level logger were barometrically compensated using a collocated Solinst Barologger Edge. Discharge values for the spring were calculated using the continuous stage data and a previously developed rating curve (Robinson and Hasenmueller, 2017).

2.3. Salt load calculations for groundwater

Load calculations for both Na^+ and Cl^- exports from the spring were performed using our weekly grab sample data. Ion loads were calculated by multiplying each ion concentration and the calculated spring discharge, averaging the values between neighboring point measurements to obtain the load over that time interval, summing all the intervals, and converting units of mass to megamole (Mmol). To understand the effects of seasonality on salt loads, we divided the dataset into four seasons defined as: winter (1 November–31 January), spring (1 February–30 April), summer (1 May–31 July), and fall (1 August–31 October). Due to this division, road salt applications during our study period occurred over two different seasons (i.e., winter and spring). To analyze annual loads, we divided the dataset into the years 2017–2018 (winter 2017–2018 to fall 2018) and 2018–2019 (winter 2018–2019 to summer 2019). Groundwater analyses ceased in July 2019 and, consequently, the annual dataset for 2018–2019 is incomplete.

2.4. Soil sampling and analysis

Soil samples were collected 1–2 m from each lysimeter nest every 3 months for 1 yr (i.e., November 2018, February 2019, May 2019, and August 2019) to evaluate changes in the soil's exchangeable ion pool (i.e., Cl^-, Na^+, Ca^{2+}, Mg^{2+}, and K^+) due to road salt applications. A hand auger was used to collect one core near each nest (A–D; four cores total for each sampling event). Core depths were slightly deeper than the deepest lysimeter depth at each nest (i.e., core depths of 25 cm for nests A and D and core depths of 55 cm for nests B and C). Cores were divided in depth intervals of 5 cm at 0–5 cm depth, then 10 cm-depth intervals after that to the greatest depth. Each subsample was stored in a sealed plastic bag at 4 °C until analysis.

Once in the laboratory, exchangeable ions were measured in triplicate for each sample by obtaining three subsamples of soil from every sealed storage bag. To measure extractable Cl^- for the soil samples, 25.0 mL of 0.01 M $CaNO_3$ was added to 10.0 g of air-dried soil (soil drying time was 3–5 days). The mixture was shaken for 15 min, and immediately gravity-filtered using a 11-μm pore size paper filter. The resulting filtrate was analyzed by IC. To determine exchangeable Na^+, Ca^{2+}, Mg^{2+}, and K^+ concentrations for soil replicates, we added 25.0 mL of 0.1 M $BaCl_2$-NH_4Cl to 3.0 g of air-dried soil for each sample, shook the mixture for 30 min, and allowed the samples to settle overnight. The following day, samples were gravity-filtered with a 11-μm pore size paper filter, then acidified to 1% HNO_3. Extracts were diluted by 1:6 to 1:12, depending on the expected concentrations. Finally, all cation extract samples were analyzed by ICP-OES. Extractable ion data are presented in mmol of ion per kg of dry soil (mmol/kg). Exchangeable cation data were used to calculate soil cation exchange capacity (CEC; $cmol_c/kg$) and ESP (%).

2.5. Statistical analyses

Statistical analyses ($\alpha = 0.05$) of the major ion concentrations in soil porewater included a one-way analysis of variance (ANOVA), used to measure the effects of distance from the road and depth on ion concentrations in soil porewater. Regression analyses were performed to determine if there were significant temporal trends in soil porewater and groundwater Na^+ and Cl^- concentrations. Regression analyses were also used to measure the relationships between Na^+ and Cl^- and other variables (e.g., spring discharge and major cation concentrations).

3. Results and discussion

3.1. Chemistry of roadside soil

3.1.1. Soil porewater

Over the monitoring period, soil porewater Na^+ and Cl^- concentrations were always higher than concentrations observed in precipitation (<0.003 mM; NADP, 2020), ranging from 0.03 mM to 9.23 mM and <0.01 mM to 15.99 mM, respectively. Soil porewater Na^+ and Cl^- were higher and more variable near the paved road, but their averages and standard deviations decreased with increasing distance from the road (Fig. 2; Table S2). At all distances from the road, changes in the relative proportions of $Na^+ + K^+$ (0.01–0.55 of the cation composition) and Ca^{2+} (0.37–0.90 of the cation composition) dominated the porewater cation chemistry, while Mg^{2+} consistently made up 0.08–0.19 of the cations. Porewaters at 1.0 m and 1.5 m from the road experienced increased Na^+ content during the winter, with porewaters 1.0 m from the road even transitioning from the Ca^{2+}-type to the Na^+-K^+-type water domain at times (Fig. 2A), despite the carbonate

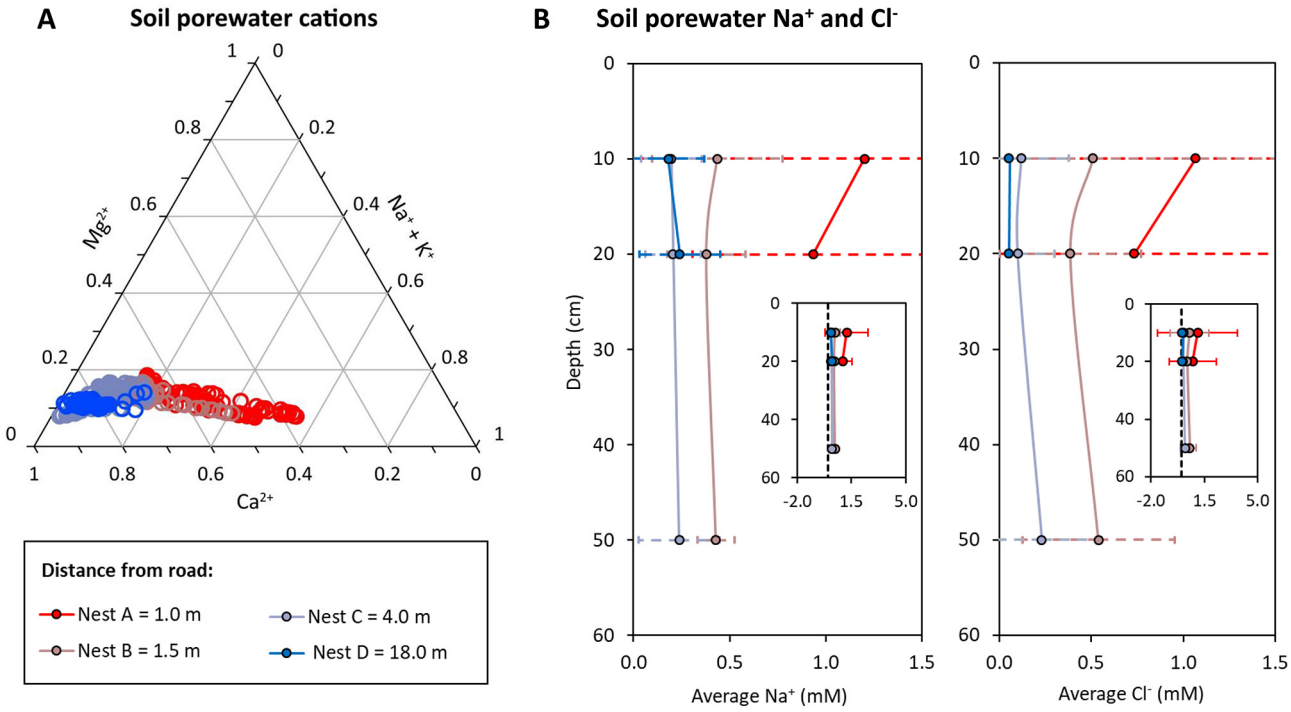

Fig. 2. A) Ternary diagram showing the relative proportions of major cations, calculated in meq/L, in soil porewater samples as a function of distance from the road. B) Average soil porewater Na^+ and Cl^- concentrations during the study period at different depths and distances from the road. Dashed bars represent standard deviations for each depth increment. The inlaid plots show the entire range of standard deviations.

lithology at the site. This gradient suggests that road salt cations reached soils up to 1.5 m from the paved road, introducing large amounts of Na^+ ions and significantly affecting the water type of soil porewaters.

With respect to depth, the highest average concentrations of Na^+ and Cl^- where found in nest A at 10 cm of soil depth (1.23 mM and 1.07 mM, respectively), where the standard deviations (1.38 mM and 2.64 mM, respectively) were higher than other sites and depths (Fig. 2B; Table S2). In nest A at 20 cm of soil depth, average Na^+ and Cl^- concentrations were lower than near the surface (0.93 and 0.73 mM, respectively). In nests B and C, Na^+ and Cl^- concentrations at all depths averaged below 0.44 and 0.54 mM, respectively. In nest D (i.e., our control group), average Na^+ and Cl^- were below 0.24 and 0.05 mM, respectively. One-way ANOVA tests showed that distance from the road had a significant effect on Na^+ and Cl^- concentrations at all studied depths ($p < 0.05$). In contrast, depth did not have a significant effect on Na^+ and Cl^- concentrations in almost all the nests ($p > 0.05$), potentially due to the high ion variability for specific samplers over time.

3.1.2. Soil exchange sites

We also studied seasonal changes in exchangeable Cl^-, CEC, ESP, and other exchangeable cations (Ca^{2+}, Mg^{2+}, and K^+) in soil collected near our porewater samplers to determine relationships between exchange site and porewater chemistries (Figs. 3, S2). Exchangeable Cl^- was consistently lowest in our control group (always ≤0.19 mmol/kg for the entire sampling period; Fig. 3). The highest values of exchangeable Cl^- (up to 1.07 mmol/kg; 680.92% higher than the control group) were detected closest to the road in both November 2018 and February 2019, coinciding with the salting period. Exchangeable Cl^- for both the November 2018 and February 2019 samples decreased with distance from the road (Fig. 3). In May 2019 and August 2019, exchangeable Cl^- values at sites near the road were much lower than those observed during the road salting period. However, Cl^- values were still higher for sites near the road than the control group during this time. Our data suggest that the soil exchangeable Cl^- pool was derived from road salting, but was rapidly and almost completely flushed from the soil once road deicing activities ceased (i.e., up to 87.1% Cl^- loss for soil samples near the road from February 2019 to August 2019). Nevertheless, the consistently higher exchangeable Cl^- values near the road compared with the control site demonstrate that there is some Cl^- retention, possibly through conservative mechanisms such as incomplete soil water flushing or non-conservative processes like anion exchange, uptake by vegetation and microbes, and chlorination of OM (Bastviken et al., 2007).

At each soil sampling site, soil CEC was similar across time for individual sampling depths. Soil CEC was also similar among the sites near the road (21.28 ± 1.36 $cmol_c/kg$), but was consistently higher in our control group (47.68 ± 6.21 $cmol_c/kg$; Fig. 3). Higher CEC at the control site was probably due to higher OM content at this location. Indeed, Robinson et al. (2017) observed ~10% higher OM content at the control site compared with sites near the road. Soil ESP was generally lowest in our control group compared to the sites near the road for any given sampling event. The ESP values were lowest and most similar among sites (0.70 ± 0.35%) in November 2018. Values of ESP increased for all sites in February 2019, but the largest increases were observed near the road, suggesting road salt contamination at these locations. Soil ESP was 8.58% in the shallowest soil near the road, compared to 2.33% at the control site for the same depth and time period. While soil ESP increased at the control site from February 2019 to August 2019, soil ESP at the surface for the site nearest to the road decreased from 8.58% to 5.05% over this period (Fig. 3). The persistence of high soil ESP values near the road in the spring and summer, compared to exchangeable Cl^- during this time, shows higher Na^+ retention in the soil. This enhanced retention until at least August 2019 suggests months-long immobilization of large amounts of road salt-derived Na^+ on cation exchange sites in the soil. Concentrations of exchangeable cations (Na^+, Ca^{2+}, Mg^{2+}, and K^+; Fig. S2) were generally higher in our control group than the sites near the road, likely due to the overall higher soil CEC at the control site. However, during the road salting period in February 2019, exchangeable Na^+ 1.0 m from the road was up to 226.81% higher than the control group. This observation further supports the

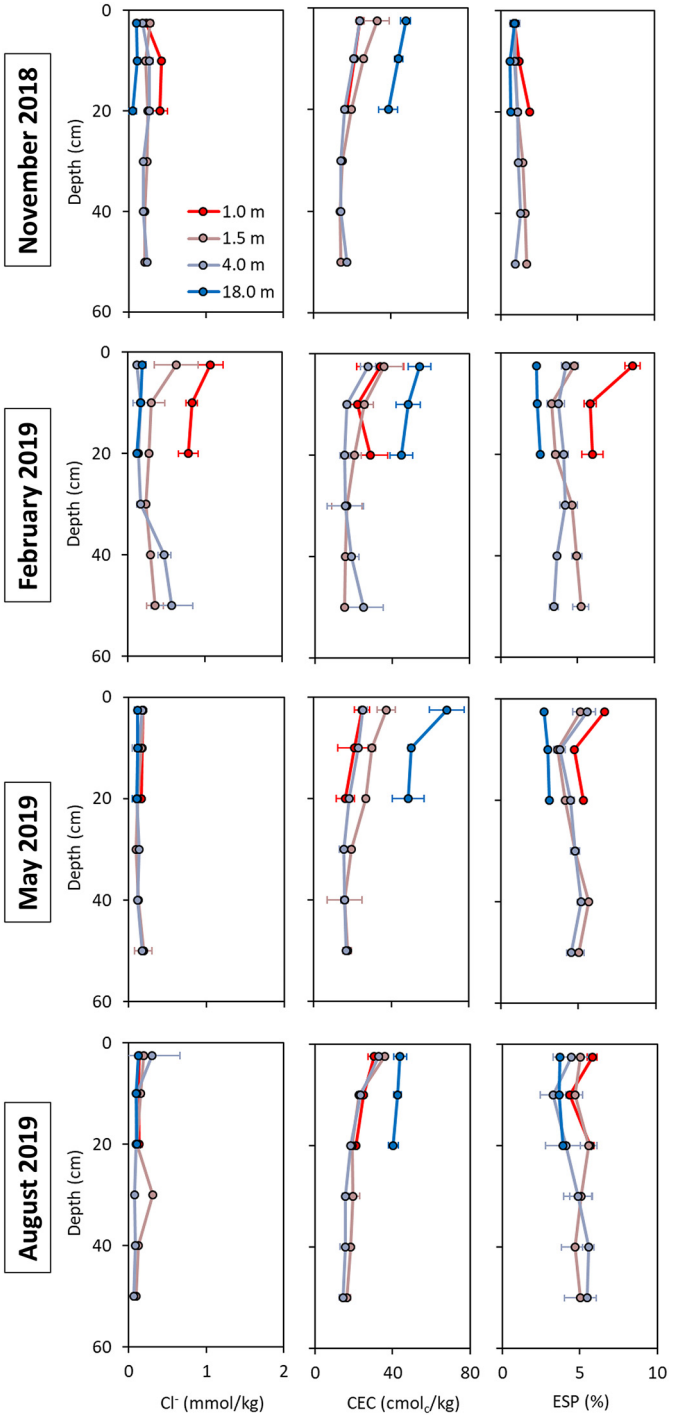

Fig. 3. Exchangeable Cl^-, CEC, and ESP data for soil cores collected quarter-annually at 1.0 m, 1.5 m, 4.0 m, and 18.0 m from the road. Each soil core corresponds to a soil porewater sampler nest (A, B, C, and D, respectively). Data from each sampling event (November 2018, February 2019, May 2019, and August 2019) are grouped in rows. Each soil depth range is represented by a symbol at the midway point for that interval. Data are shown as averages for each triplicate measurement, and bars represent the standard deviations for the triplicate samples.

enhanced adsorption of Na^+ onto soil exchange sites triggered by the introduction of large amounts of Na^+ from salt-laden road runoff. While we observed increased exchangeable Na^+ concentrations near the road during the salting period, we did not observe any corresponding concentration decreases for other exchangeable cations (e.g., Ca^{2+}, Mg^{2+}, or K^+) during this time. Nevertheless, we observed that the percentages of exchangeable Ca^{2+}, Mg^{2+}, and K^+ relative to CEC decreased near the road in February, coinciding with high road salt application rates and elevated ESP values. This observation suggests that, when large amounts of Na^+ are introduced to the system, other exchangeable cations present in the soil are likely being released from soil exchange sites.

3.2. Salt retention mechanisms in roadside soil

3.2.1. Slow porewater movement

We examined temporal changes in soil porewater Na^+ and Cl^- over the monitoring period (Fig. 4) to understand salt retention mechanisms in soils. In our control group, porewater Na^+ and Cl^- levels remained consistently below 1.20 mM throughout the study. Moreover, during the road salting period, Na^+ and Cl^- values at the control nest were always <0.50 mM (the lowest values of any site and lower than values at the control site in the late summer), demonstrating that road salts did not reach nest D.

Following the 2017–2018 road salting period, Na^+ and Cl^- concentrations were elevated near the road but decreased rapidly to <0.50 mM for all sites during the wetter, early spring months. High porewater Na^+ and Cl^- concentrations detected during the summer and early fall (May to early November 2018) occurred before the beginning of the road salting period in all nests, including our control group (Fig. 4). During this period, increases in other cations were also observed in all sites (e.g., Ca^{2+}, Mg^{2+}, K^+, and Si^{4+}; Figs. S3–S6). The peaks coincided with a drier period from 1 May to 30 September 2018 when precipitation was 8.5 cm/month (2.0 cm below the monthly average; Fig. 4E) and evapotranspiration (ET) was high (Criss and Winston, 2008). The drier conditions led to soil moisture depletion, causing low sample recovery during this time period. Soil porewater Na^+ and Cl^- levels for all the samplers peaked after the summer dry period on 10 November, 5 days before the first road salt application of the season on 15 November (see Fig. S7 for details on sample timing in relation to precipitation amounts and road deicing applications). We attribute these pre-road salting ion peaks observed in all the samplers (including the control site) in early November to a first flush event that mobilized salts accumulated during the drier summer and early fall months. Indeed, these salt peaks in all soil porewater samples followed fall leaf drop and several rainfall events in early November (Figs. 4E, S7), which could have mobilized ions and replenish the soil water. Given that the response occurs before road salting, the November increases in soil porewater ions cannot be the result of road salt applications.

To estimate the rates of lateral and vertical transport of road salts through soils for the road salting period, we compared the timing of consecutive Na^+ and Cl^- peaks in porewater at increasing distances from the road and depths. The highest concentrations of Na^+ and Cl^- (9.23 and 15.99 mM, respectively) were detected on 18 January 2019 at 10 cm of soil depth 1.0 m from the road (Fig. 4A), 7 days after the largest road salt application of the 2018–2019 road salting period (see Fig. S8 for details on sample timing in relation to precipitation amounts and road deicing applications). A second set of peaks in Na^+ and Cl^- concentrations was observed 8 March 2019, which occurred 5 days after a road salt application on 3 March 2019 (Fig. 4A; see Fig. S9 for timing details). This 5- to 7-day delay in the Na^+ and Cl^- concentration peaks in our shallowest sampler at 1.0 m from the road is likely due to a combination of gradual snowmelt mobilizing salt ions as well as slow porewater transport through the soil. However, differentiating the melt delay timing from the soil porewater flow timing near the road is challenging. The exact snowmelt delay timing varies among snowfall events due to temperature, snow thickness, vegetative shading, and the form and timing of subsequent precipitation events. For instance, maximum daily temperatures were slightly above 0 °C during and immediately following the snow event in January, likely inducing some snowmelt, but the thick snowfall (~200 mm; Fig. S8) likely prevented rapid snowmelt. In contrast, temperatures after the snow

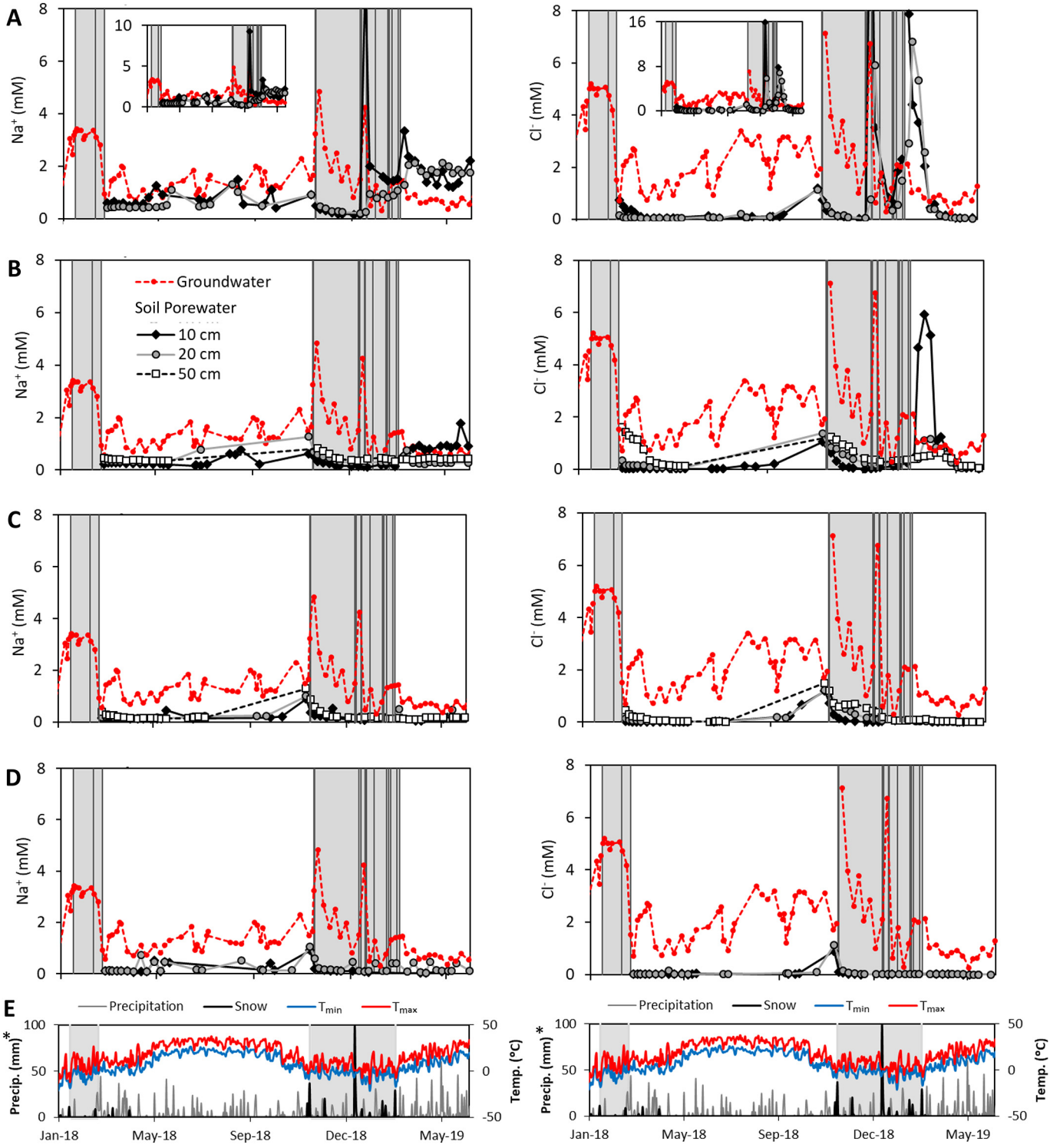

Fig. 4. Soil porewater (gray-scale symbols and lines) and groundwater (red symbols and lines) Na^+ (right column) and Cl^- (left column) concentrations over time. Soil water sampler nests are grouped in rows A, B, C, and D (1.0 m, 1.5 m, 4.0 m, and 18.0 m from the road, respectively). Porewater data are shown for samplers at 10 cm (diamonds), 20 cm (circles), and 50 cm (squares) of soil depth. The shaded regions highlight road salting periods and dark gray vertical lines within these periods represent specific road salt application events. Embedded plots for nest A show the large concentration maxima for Na^+ and Cl^- during road salting events. Row E shows climate data during the study period. The axis labeled "Precip.*" indicates both the daily total precipitation in water equivalents (gray), which includes all forms of precipitation, and snowfall values (black), which are divided by two so that they fit on the axis. Minimum (T_{min}; blue) and maximum (T_{max}; red) air temperatures are also shown. For interpretation of the references to color in this figure, the reader is referred to the web version of this article.

event on 3 March remained below 0 °C until 6 March, but the much thinner snowpack (~59 mm; Fig. S9) might have promoted faster snowmelt once temperatures were above 0 °C. Despite the uncertainty associated with melt timing, our data suggest that melting began to occur within 3 days of each event. If we assume at least 3 days before meltwaters enriched in salt reach the soil nearest to the road, then lateral salt movement through the soil near the road occurred at a rate of approximately 25 to 50 cm/day.

To investigate delays in salt transport solely due to slow porewater movement through the soil (without the confounding factor of melt timing), we investigated the timing between peaks detected in our porewater samplers 1.0 m and 1.5 m from the road because we know that melt had already occurred to reach the 1.0 m sampler. While we did not observe any ion peaks in the 1.5 m sampler following the road salting events that commenced on 11 January 2019, a peak in porewater Cl^- content (5.93 mM) was detected at 10 cm of soil depth 1.5 m from the road on 21 March 2019, 13 days after the 8 March 2019 peak observed 1.0 m from the road at the same depth (Fig. 4A–B). This delayed peak indicated that lateral movement of Cl^- slowed to 3.9 cm/day at greater distances from the road. Porewater Na^+ peaks were not observed 1.5 m from the road, suggesting slower, non-conservative Na^+ transport through the soil compared to Cl^- (Fig. 4B).

Vertical movement of water through the soil also slowed salt transport. Salt peaks of 0.93 mM and 5.91 mM for Na^+ and Cl^-, respectively, were detected on 23 January 2019 at 20 cm of soil depth in nest A (Fig. 4A). These ion peaks followed the salt increase detected on 18 January at 10 cm depth in nest A, indicating vertical salt transport of 2.0 cm/day at 1.0 m from the road. The same 5-day vertical delay at nest A was observed between ion peaks following the 3 March 2019 salting event (i.e., ion peaks on 8 March 2019 for the 10 cm sampler and 13 March 2019 for the 20 cm sampler). While nest B did not respond to the 11 January 2019 salting event (Fig. 4B), ion peaks were observed following the 3 March 2019 salting event. Following the Cl^- peak at 10 cm depth for nest B on 21 March 2019, we detected Cl^- peaks of 1.17 mM at 20 cm and 0.63 mM at 50 cm of soil depth on 29 March 2019 and 11 April 2019, respectively. This response indicates a vertical salt transport of 1.3 cm/day from 10 cm to 20 cm of soil depth and 2.3 cm/day from 20 cm to 50 cm of soil depth. No Na^+ maxima were observed in nest B (Fig. 4B), indicating again that Na^+ is less mobile compared to Cl^-. In nests C and D, no road salt-related peaks were detected (Fig. 4C–D).

Our findings of faster salt transport rates closer to the road and more rapid salt delivery through the soil surface are consistent with stable isotope ($\delta^{18}O$ and δ^2H) results from soil porewater and groundwater. All soil porewater and groundwater samples were meteoric in origin as they plotted along the global meteoric water line (MWL; Fig. S10). In other words, they displayed no evidence of significant evaporation or water-rock interactions, both of which can enhance ion content in the water.

The overall variability of the isotopic composition of soil porewater and groundwater can be used to estimate water residence times within a given reservoir (Mueller et al., 2014; Thomas et al., 2013). Highly variable water isotope values at a given location and depth are generally associated with shorter residence times. In contrast, lower variability of isotopic signals indicates longer residence times. We observed that the $\delta^{18}O$ and δ^2H standard deviations of soil porewaters decreased with distance from the road, indicating that soil water flow was rapid near the road, but flow slowed with increasing distance from the roadway (Fig. S11; Table S3). One exception was our control group at nest D, which had the highest isotopic variability of all the nests. The control site was located on a steep slope that decreased water retention times and thereby increased isotopic variability. We also observed that soil porewater isotope compositions near the surface were lighter and more variable compared with the deeper portions of the soil profile (Fig. S11; Table S3). Indeed, the standard deviation of $\delta^{18}O$ in soil porewater was, on average, 31.0% lower at depths of 50 cm compared to 10 cm, even when accounting for differences in sample size between depth intervals (i.e., we only included samples for the comparison when we could collect samples from all soil depth intervals). The groundwater $\delta^{18}O$ composition was notably heavier ($-6.98 \pm 0.72‰$) than soil porewater ($-7.71 \pm 2.17‰$; Table S3). The lighter isotopic signature in the vadose zone, especially near the soil surface, was the result of our sampling occurring predominantly during winter months when local precipitation generally has more depleted isotope values (Criss, 1999), as well as our inability to collect isotope samples during the summer due to limited soil porewater volumes (i.e., lysimeters had <10 mL of water). In contrast, groundwater was sampled equally across seasons. The overall decrease in isotopic variability with depth that we observed is expected due to longer residence times and enhanced mixing (Table S3; Thomas et al., 2013).

Our isotope results confirm that salt contamination from deicing applications moves rapidly with porewaters near the road and at the surface, but is slowed by the reduced physical movement of porewaters away from the road and deeper in the vadose zone and, eventually, the phreatic zone. Indeed, we found that porewater Na^+ and Cl^- peaks decreased in concentration with distance from the road and depth, supporting the occurrence of hydrodynamic dispersion and diffusion. Once we determined the salt transport rate through the soil, we estimated the rate at which a salt plume originating at the soil surface would reach the water table. Previous isotope hydrologic studies (Frederickson and Criss, 1999) and the presence of a karst spring at this site suggest that the local water table is relatively shallow at our sampling site. We estimated that the local water table depth was between 50 cm and 100 cm below the ground surface near our samplers. Using the range of our estimated vertical salt movement (i.e., 1.3 cm/day to 2.3 cm/day), porewater vertical migration alone would delay the arrival of the salt plume to the groundwater for at least 22–77 days. However, our salt delivery approximations likely underestimate the delayed delivery of road salts to groundwater across the spring's catchment because the water table could be considerably deeper at other locations in the recharge area and porewater retention times likely increase with depth (as we observed for our ion and isotope data, where variability attenuated with increasing depth in both cases; Figs. 2B, S11). Furthermore, rates of porewater movement in the vadose zone are highly dependent on saturation conditions, which can vary depending on recent precipitation inputs and soil characteristics.

3.2.2. Ion exchange reactions

Our soil porewater results also showed evidence for a second salt retention mechanism, ion exchange, which has been suggested by previous studies (Moore et al., 2017; Rhodes and Guswa, 2016; Robinson et al., 2017; Rossi et al., 2017). Ion exchange processes mostly affect cations (e.g., Na^+). Halide ions, such as Cl^-, tend to behave more conservatively, migrating through systems with minimal interaction with substrates. While previous studies have demonstrated temporary retention of Cl^- in soils via uptake by microbes or plants, sorption on soil particles, and chlorination of OM (Bastviken et al., 2007; Kincaid and Findlay, 2009), these processes have limited impact on overall Cl^- transport through the soil (Robinson et al., 2017). In our study, we observed overall higher exchangeable Cl^- content in the soil at sites near the road, even well after the road salting period (Fig. 3), suggesting the possibility of some Cl^- retention. However, our study does not allow us to differentiate between non-conservative Cl^- retention mechanisms. Multiple mechanisms could contribute to non-conservative Cl^- retention in our study, but the generally rapid movement of Cl^- observed through our soil sites (Figs. 3, 4) suggest relatively conservative behavior compared with Na^+.

Our soil chemistry results clearly demonstrated soil Na^+ retention via cation exchange. We observed an increase in soil ESP near the road following road salt applications, indicating the sorption of relatively high amounts of exchangeable Na^+ onto cation exchange sites (Fig. 3). Following both road salting periods, we observed elevated soil porewater Na^+ levels in samplers near the road well after the cessation of road salt applications (Fig. 4). Immediately after the milder 2017–2018 winter, Na^+ concentrations 1.0 m from the road remained below ~0.50 mM, but started increasing above 0.50 mM in early spring and remained relatively high until the start of the 2018–2019 road salting period. In contrast, Na^+ concentrations at the control site, 18.0 m from the road, were much lower (~0.10 mM) in the 2 months after the 2017–2018 road salting season. After the snowier 2018–2019 winter, porewater Na^+ levels were ~3.5× higher than the previous non-

salting period at nest A, averaging at 1.84 mM (Fig. 4A). Soil porewater Na^+ concentrations systematically decreased away from the road and were nearly always <0.50 mM at nests C and D after the 2018–2019 salting period. We attribute elevated, non-salting period soil porewater Na^+ concentrations near the road to the release of previously retained Na^+ ions due to cation exchange reactions with soil particles. These soil cation exchange reactions triggered by road salting events were evidenced by the changes in relative proportions of major cations normalized to CEC at the site 1.0 m from the road. As an example, for shallow soil samples collected before road salt applications in November 2019, Ca^{2+} made up 87.45% of the cations on exchange sites, yet Ca^{2+} concentrations in soil porewaters were relatively low during this time (Fig. S3). In February 2019, when deicer applications were performed, Ca^{2+} concentrations in soil porewaters in nest A increased >2× (Fig. S3), while the relative proportion of Ca^{2+} on soil exchange sites decreased to 81.93%.

Cation exchange reactions due to excess Na^+ in the soil were further supported by the comparison of molar cation (e.g., Na^+, Ca^{2+}, Mg^{2+}, and K^+) and Cl^- ratios (Meriano et al., 2009) measured in soil porewater during the 2018–2019 road salting period (Fig. 5). Using the Na^+ and Cl^- concentrations from the road salt sample, we determined the expected molar Na^+:Cl^- ratio if no cation exchange processes occurred within the soil. Given that Na^+ represents 95.4% of the total cations in the salt sample (Table S4), the Na^+:Cl^- line for the deicing salt plots slightly below a 1:1 ratio (Fig. 5). For the analysis of Na^+:Cl^- ratios in the soil porewaters, we used the ion concentrations

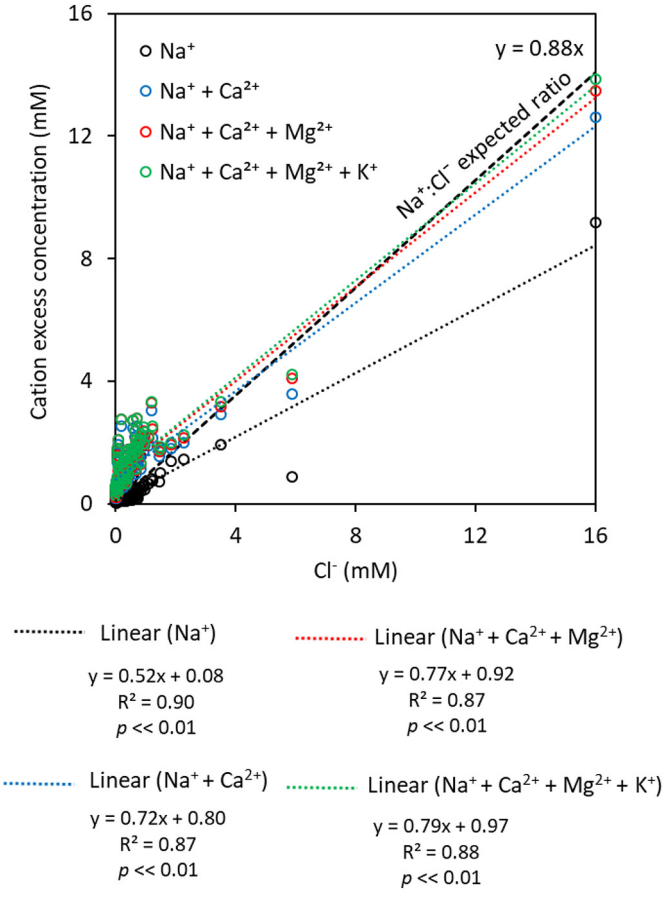

Fig. 5. Molar concentrations of Na^+ (black) and Na^+ accumulatively paired with the exchangeable cations Ca^{2+} (blue), Mg^{2+} (red), and K^+ (green) plotted against Cl^- measured in soil porewaters from nests A-C (normalized to the nest D control site) during the road salting period. The dashed black line indicates the expected Na^+:Cl^- ratio (0.88) for the deicing salt applied at the study site. For interpretation of the references to color in this figure, the reader is referred to the web version of this article.

detected in nests A-C during the 2018–2019 salting period, when excess Na^+ is introduced to the system and would be expected to displace other cations on exchange sites. To get each of the cations' excess concentrations, we subtracted the respective "background" concentrations in soil porewater for each ion. We defined the soil porewater "background" cation concentrations as the average ion concentrations detected in our control group (nest D) during the same salting period. We note that CEC and, thus, exchangeable cation concentrations in soil samples collected near nest D were generally higher than the other sites across time (Figs. 3, S2). Higher CEC for the control site was likely due to differences in soil type at this location. However, this difference in CEC between the control site and the sites near the road does not necessarily mean that nest D porewater chemistry is not representative of the "background" cation composition of the porewaters at the other sites. If cations in soil porewaters are at equilibrium with those on exchange sites, "background" porewater chemistry should be similar among sites.

The soil porewater Na^+:Cl^- line (m = 0.52; $p \ll 0.01$; black symbols in Fig. 5) for nests A-C during the road salting period plots well below the expected Na^+:Cl^- ratio for the deicing salt (m = 0.88), indicating Na^+ retention in the soil relative to Cl^-. This trend is partially driven by samples with relatively high Cl^- that correspond to porewaters near the road collected immediately following road salt applications. Depletion of Na^+ relative to Cl^- in the porewater agrees with our exchangeable ion analyses from the soil cores, where we observed nearly complete Cl^- loss from the soil soon after road salt applications, while Na^+ stayed on soil exchange sites for an extended period (Fig. 3). To identify the cation excess due to the potential release of Ca^{2+}, Mg^{2+}, and K^+ after displacement by Na^+ ions from road salt, we compared the "missing" concentrations of Na^+ to the observed Ca^{2+}, Mg^{2+}, and K^+ concentration excesses in soil porewater during the 2018–2019 salting period (Fig. 5). These excess cation concentrations were cumulatively added to the corresponding porewater Na^+ concentration, then plotted against molar Cl^-. As each major cation value was added to porewater Na^+ levels, the slope moved closer to the expected Na^+:Cl^- ratio for the deicing salt. When all the major cations we measured were included in the analysis, the slope of the best fit line (m = 0.79) was similar to the slope for the Na^+:Cl^- ratio in the deicing salt (m = 0.88). This relationship suggests release of soil Ca^{2+}, Mg^{2+} and K^+ in exchange with Na^+ originating from road salt (Fig. 5). Ion exchange processes triggered by deicing applications can lead to ecosystem degradation in soils including the loss of plant-related nutrients (e.g., K^+), the development of sodic soils (Asensio et al., 2017), and the mobilization of toxic trace elements to porewaters (Bäckström et al., 2004; Nelson et al., 2009; Wilhelm et al., 2019) that may subsequently reach groundwaters.

To investigate the timing of non-conservative Na^+ retention in soils, we evaluated the seasonality of the Na^+:Cl^- ratio for our soil porewater samples (Fig. 6). We observed that the Na^+:Cl^- ratio in the nest D control group was always above the expected 0.88 ratio in road salts, indicating an excess of Na^+ compared to Cl^- in the unimpacted soil porewater. We do not expect that this site has received road salts due to its distance from the road and location on a forested slope towards the road. We also note that atmospheric inputs of Na^+ and Cl^- to the study site were low at <0.003 mM (NADP, 2020). Relatively high Na^+ compared to Cl^- in the control group may therefore be due to higher Na^+ availability from weathering of minerals present at the site or loss of mobile Cl^- over time, though detailed mineralogical data for the soil and host rock at the study site are unavailable. In nests A-C, however, we commonly observed Na^+:Cl^- ratios below the expected value of 0.88, especially following road salt applications in the winter and into the early spring months. During this time, porewaters featured excess Cl^- relative to Na^+, indicating Na^+ retention on cation exchange sites. By ~1.5 months after the road salting period, porewater Na^+:Cl^- ratios increased above 0.88, indicating that Cl^- had largely been lost from exchange sites and the porewater solution, while Na^+ was still

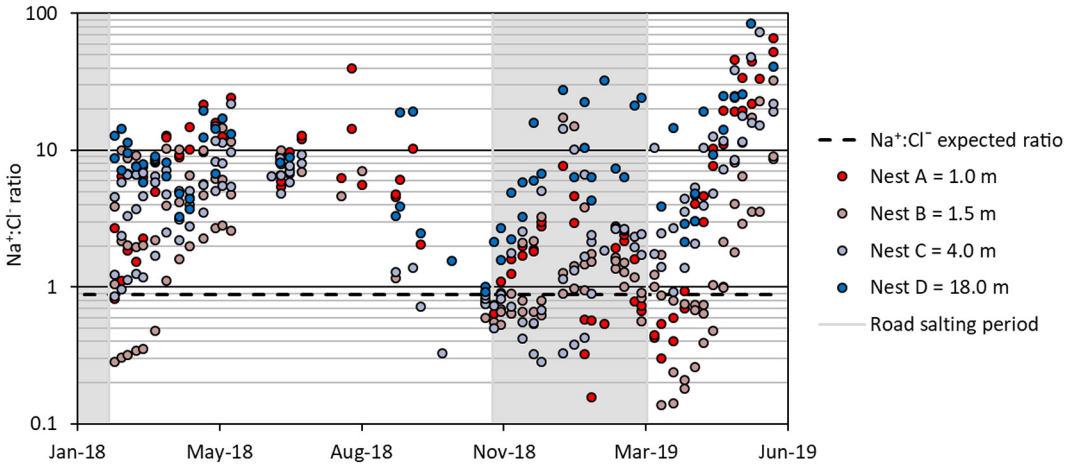

Fig. 6. Soil porewater Na^+:Cl^- ratios (logarithmic scale) for nests A-D (1.0 m, 1.5 m, 4.0 m, and 18.0 m from the road; red to blue gradient) as a function of time. The dashed black line indicates the expected Na^+:Cl^- ratio (0.88) for the deicing salt applied at the study site. Gray shaded areas indicate road salting periods. For interpretation of the references to color in this figure, the reader is referred to the web version of this article.

present on exchange sites and being released into the porewater. This seasonal porewater effect is consistent with our exchangeable Cl^- and ESP results from our soil samples, which showed near complete Cl^- loss by May 2019, but Na^+ retention well into the summer (Fig. 3). The Na^+:Cl^- ratio began to decrease by mid-summer (Fig. 6), about 5 months after the end of road salt applications. We attribute this decrease in the Na^+:Cl^- ratio to the gradual loss of Na^+ from soil exchange sites as evidenced by decreasing ESP following the end of road deicing activities (Fig. 3). Our results agree with previous Na^+ retention estimates from laboratory flushing experiments using soils from this site (Robinson et al., 2017).

We also explored the timing of other exchangeable cation (Ca^{2+}, Mg^{2+}, and K^+) releases to soil porewater due to exchange with Na^+ following salt applications (Figs. S3–S5). During the 2018–2019 salting period, we observed that maxima for these cations occurred concomitantly to the arrival of salt-laden soil porewater to nest A (e.g., see peaks for the 10 cm samplers on 18 January 2019 for all cations). This indicates that increases in these ions were related to road salt applications. We did not observe peaks in these cations at greater distances from the road, which corresponds to our observation of no winter Na^+ concentration peaks for these samplers. In the United States, NaCl is the most frequently used deicing salt because it is common and inexpensive. However, $CaCl_2$, $MgCl_2$, and KCl can also be used as deicing agents. The road salt sample we collected on site did contain some Ca^{2+} and Mg^{2+} (<2.2 wt%), but the proportions were very low compared to Na^+ (33.9 wt%) and Cl^- (59.4 wt%; see Supplemental material Section 2.1 and Table S4 for details on the road salt composition). The relative proportions of other cations compared to Na^+ are too low in the road salt to account for their portions in soil porewaters relative to Na^+ observed after road salting events (see Supplemental material Section 2.1 for further details). Thus, increased cation concentrations are likely mainly the result of cation release from exchange with Na^+ ions from road salt application.

3.3. Chemistry of groundwater

Our weekly grab samples from the groundwater-fed karst spring had respective average Na^+ and Cl^- concentrations of 1.58 mM and 2.33 mM (Table S2). The highest grab sample Na^+ and Cl^- concentrations were detected during the winter, while the lowest ion levels were measured during the spring months (Fig. 7). We observed that grab sample Cl^- values (measured on an IC) exceeded the United States Environmental Protection Agency (USEPA) chronic toxicity threshold of 230 mg/L (6.48 mM) two times during the 2018–2019 road salting period. Our continuous Cl^- dataset showed an increase over the USEPA chronic toxicity threshold that occurred in August

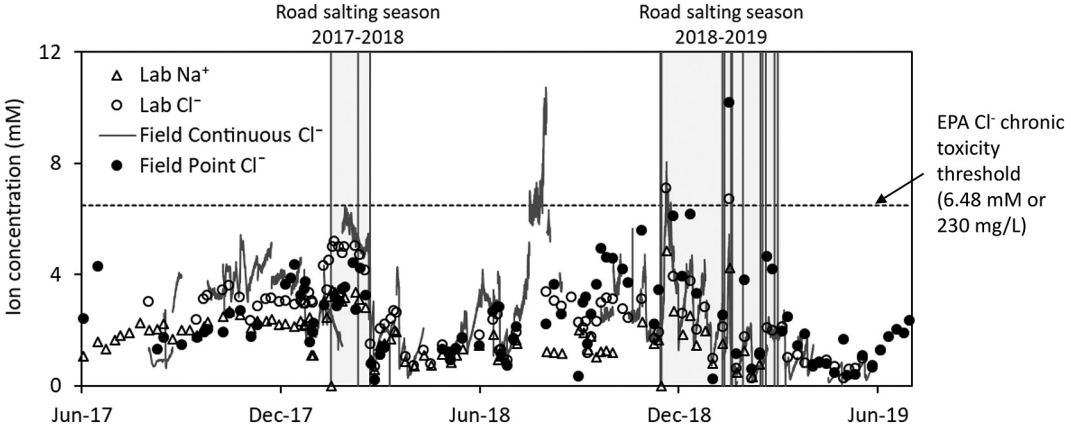

Fig. 7. Shallow groundwater point measurements of Na^+ (triangles) and Cl^- (circles) concentrations over time. White shapes represent laboratory results from physical grab samples collected at the spring. The black circles are field Cl^- measurements and the solid gray line shows the continuous Cl^- dataset (see Fig. S12 for a comparison of laboratory and field Cl^- data). The USEPA chronic toxicity threshold for Cl^- (6.48 mM or 230 mg/L) is indicated with a dashed black line.

2018, but these high concentrations were not detected in the laboratory analyses of water samples. The correlation between Cl^- field and laboratory data suggests that the field devices do not always accurately estimate Cl^- concentrations in the spring water (Fig. S12). The spring's Cl^- levels in grab samples increased significantly over the period between the 2017–2018 and 2018–2019 road salting periods ($p < 0.05$; Fig. 7), indicating rapid flushing of Cl^- from soils after road salt applications but subsequent Cl^- increases that were likely due to the drier conditions during the summer and early fall. In contrast, Na^+ concentrations did not change significantly between the two salting periods ($p = 0.10$; Fig. 7), again suggesting enhanced Na^+ retention in the watershed compared to Cl^-.

To differentiate between the changes in Na^+ and Cl^- concentrations in the spring due to deicing applications versus natural responses due to precipitation, ET, and weathering, we compared the results obtained from our weekly grab samples to discharge data from the karst spring. During the non-salting period, Na^+ and Cl^- concentrations were driven by dilution effects when the spring's discharge increased. This was evidenced by the negative correlation between Na^+ and Cl^- and discharge ($R^2 > 0.53$; $p \ll 0.01$; Fig. S13). During periods of deicing applications, Na^+ and Cl^- concentrations were higher and, while their correlations with discharge were still significant, they became more variable ($R^2 < 0.27$; $p < 0.02$; Fig. S13). Thus, during salting periods, Na^+ and Cl^- levels were more influenced by changes in chemistry of recharge waters rather than dilution effects due to increases in discharge.

We found that groundwater cation chemistry was dominated by changes in the relative proportions of Na^+ and Ca^{2+} (Fig. S14), which corresponds to our findings for soil porewaters (Fig. 2A). During periods when there was no road salting, groundwater chemistry fell within the Ca^{2+}-type water domain. In contrast, during periods of salting, groundwater chemistry occasionally moved closer to the Na^+-K^+-type water domain despite the carbonate lithology of the aquifer. These changes in the relative proportions of Na^+ and Ca^{2+} ions indicate that, during deicing periods, road salt contributions substantially modified the groundwater chemistry.

3.4. Transport of road salt contamination from soils to groundwater

To evaluate salt transport between different hydrological reservoirs, we compared Na^+ and Cl^- concentrations in both soil porewater and shallow groundwater. Average Na^+ and Cl^- concentrations were lower in soil porewaters (0.47 mM and 0.40 mM, respectively) compared to shallow groundwater (1.58 mM and 2.33 mM, respectively; Table S2). We observed that, during the non-salting period in 2018, the karst spring had overall higher Na^+ and Cl^- concentrations compared to all soil porewater (Fig. 4). During the 2018–2019 salting period, while the spring generally responded to road salt applications with nearly the same timing as the soil porewater near the road, its response was more attenuated (Fig. 4A). In one case (i.e., 20 November 2018), however, spring Na^+ and Cl^- peaked, but no concurrent peaks were observed in the soil porewaters (Fig. 4). Two deicing applications were performed on 15 and 16 November 2018, which were prior to the maxima in the spring (Fig. S7). These applications were relatively small and conducted by MDC employees at the Rockwoods Reservation rather than the road deicing company that normally performs salt applications for the property. The two November 2019 applications may not have been near our soil water samplers and, consequently, we did not see a direct response in our soil porewater data. The applied salts could have entered the aquifer somewhere else in the recharge area, causing an increase in ion concentrations in the spring, but not the soil porewater sites.

We compared the Na^+:Cl^- molar ratios in all soil porewater and groundwater samples (i.e., both during and after road salting events; Fig. 8). The Na^+:Cl^- values for both soil porewater and groundwater plot below the expected Na^+:Cl^- ratio line ($m = 0.88$), with slopes of 0.40 and 0.60, respectively. Slopes <0.88 demonstrated that there were higher concentrations of Cl^- compared to Na^+ for both water types, indicating Na^+ retention within each reservoir. Lower Na^+:Cl^- ratios for soil porewater compared to groundwater suggest that, during the studied period, soils retained more Na^+ than the aquifer (Fig. 8). The lower Na^+ retention observed in the groundwater indicates that other mechanisms exist that contribute to the rapid delivery of Na^+ to the spring outlet. While soils likely delay the arrival of salt ions to the aquifer, the presence of karst conduit openings (e.g., sinkholes), which connect the aquifer directly with the surface, are almost certainly causing the apparent lower Na^+ retention of the groundwater.

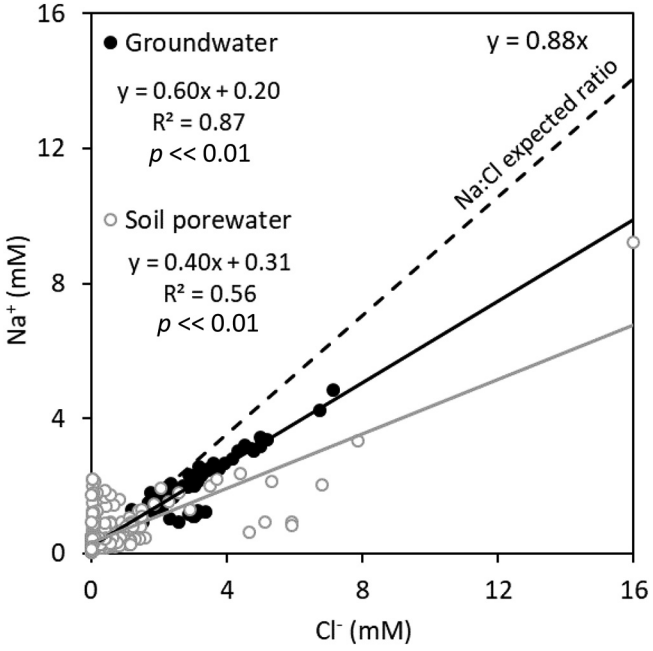

Fig. 8. The relationship between Na^+ and Cl^- concentrations in soil porewater (white symbols and gray solid line) and shallow groundwater (black symbols and black solid line). The dashed black line indicates the expected Na^+:Cl^- ratio (0.88) for the deicing salt applied at the study site.

The range of $Na^+ + K^+$ proportions in soil porewater (0.01 to 0.55; Fig. 2A) was larger than the range in groundwater (0.11 to 0.48; Fig. S14), showing that changes in Na^+ levels were more attenuated in groundwater compared to soil porewater. We also saw Na^+ and Cl^- concentration peaks in the groundwater that generally had lower amplitudes than those in the soil porewater nearest to the road (Fig. 4). These observations imply that, while a portion of the salt ions were likely being transported via faster flow paths (e.g., karst conduits) into the aquifer, other processes buffered the road salt-related contamination that reached the karst spring outlet. These buffering processes that reduce the amplitude of salt pulses in the spring likely include: 1) mixing processes between the salty recharge water and older, more dilute conduit or matrix water within the karst aquifer, 2) dilution of the salt signature due to aquifer recharge in areas not affected by road salts, and 3) road salt ion retention within soils due to slow porewater movement and ion exchange reactions and subsequent Na^+ release months later. Thus, while a previous study estimated an overall residence time of 1 yr for the aquifer that feeds Rockwoods Spring (including both matrix and conduit flow; Frederickson and Criss, 1999), diffuse flow is likely much slower than this estimate, leading to salt accumulation in the aquifer.

To better understand salt accumulation in the karst aquifer over seasonal and annual timescales, we compared estimated salt applications (details for this estimation are provided in Supplemental material Section 1.2) in the recharge area (Fig. 1) to the calculated salt exports from our spring water chemistry and discharge data. We found that

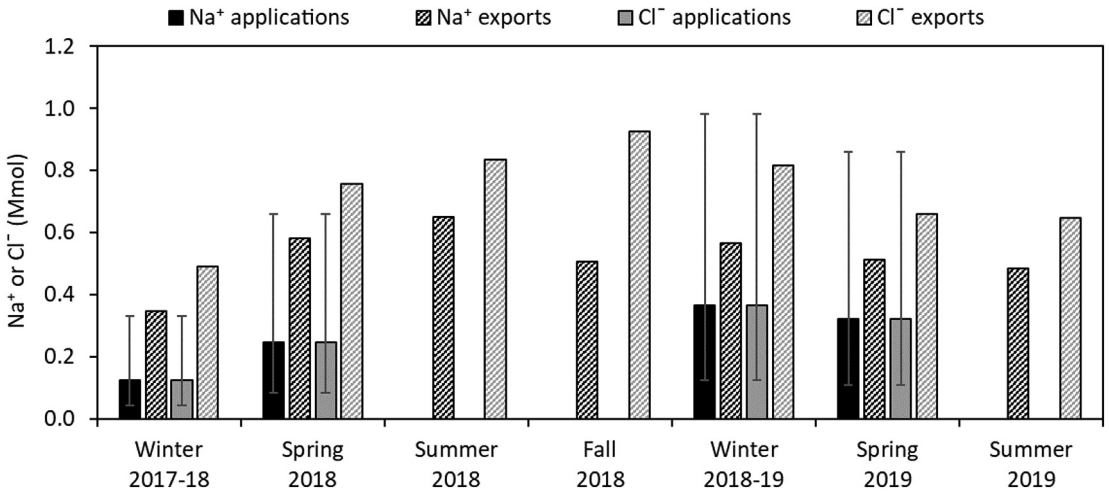

Fig. 9. Seasonal Na^+ (black) and Cl^- (gray) estimated applications (solid bars) and calculated exports (striped bars) for the karst spring. Thin black bars for the estimated application rates show the upper and lower boundaries when assuming salting outside of the Rockwoods Reservation occurred at double and half of the rate performed within the park, respectively.

both Na^+ and Cl^- exports were generally much higher than the inputs for the aquifer both seasonally and annually (Figs. 9–10), except for the upper Na^+ input estimates for the 2018 spring season (Fig. 9), the upper Na^+ and Cl^- input estimates for the 2018–2019 winter and 2019 spring seasons (Fig. 9), and the upper Na^+ input estimates over the year in 2018–2019 (Fig. 10). Seasonally, exported Na^+ and Cl^- loads were lowest during the 2017–2018 winter (0.35 and 0.49 Mmol, respectively). The highest Na^+ loads were calculated in summer 2018 (0.65 Mmol), while the highest Cl^- loads occurred later in fall 2018 (0.93 Mmol). Seasonal Na^+ exports were lower and less variable (average 0.52 ± 0.10 Mmol) than Cl^- exports (average 0.73 ± 0.15 Mmol; Fig. 9). Likewise, at the annual scale in 2017–2018, total Na^+ exports were 30.8% lower than the total Cl^- exports despite the equal total applications for both salt ions (i.e., 0.37 Mmol). For the available 2018–2019 dataset, Na^+ exports were 26.4% lower than the total Cl^- exports (Fig. 10). Higher Cl^- compared with Na^+ exports in the karst spring again suggests more conservative transport of Cl^- and retention of Na^+ along the flow path.

These findings of higher salt outputs than inputs for Rockwoods Spring (Figs. 9–10) are similar to previously reported Cl^- load data for the spring system (Robinson and Hasenmueller, 2017), but we now demonstrate that the same trends occur with Na^+ ions. Overall lower observed salt inputs than outputs for the spring is nevertheless surprising, and may be due to several factors. First, we may have underestimated road salt applications outside of the Rockwoods Reservation, despite the assumption that application rates outside of the park may be double those inside the park. Municipal deicer application rates may be much higher than the application rates used by land management-focused government agencies like MDC, who oversee the Rockwoods Reservation. In addition, private application rates are highly variable and extremely difficult to estimate, and previous studies have shown that private applications often exceed the application rates for public roads (Sassan and Kahl, 2007). However, the estimation of upper and lower boundaries of private applications as half or double the municipal application rates has been widely used in multiple past studies that have performed these estimations (Howard and Haynes, 1993; Meriano et al., 2009; Robinson and Hasenmueller, 2017; Sassan and Kahl, 2007). Second, we used Robinson and Hasenmueller's (2017) estimate of the spring's recharge area, which was based on a recharge area-discharge relationship for springs in Missouri (Criss, 2010) and the assumption that the water table generally mimics the shape of the local topography. Nevertheless, the phreatic divides for aquifers do not necessarily correlate with topographic divides, especially for karst systems. To account for this issue, Robinson and Hasenmueller (2017) tested if land cover changed substantially when a random square with the same total area was assigned as the spring's recharge area. They found that land cover did not change more than 1% when they did this test, but the randomly assigned square may still not have been representative of the true recharge area for the spring. Third, Na^+ and Cl^- may be accumulated from previous years, delaying the delivery to the spring. Indeed, long-term (1996 to 2016) Cl^- accumulation in the watershed has been demonstrated by previous studies (Robinson and Hasenmueller, 2017), suggesting that ion retention in the aquifer is likely one of the drivers of the higher salt exports observed in the spring.

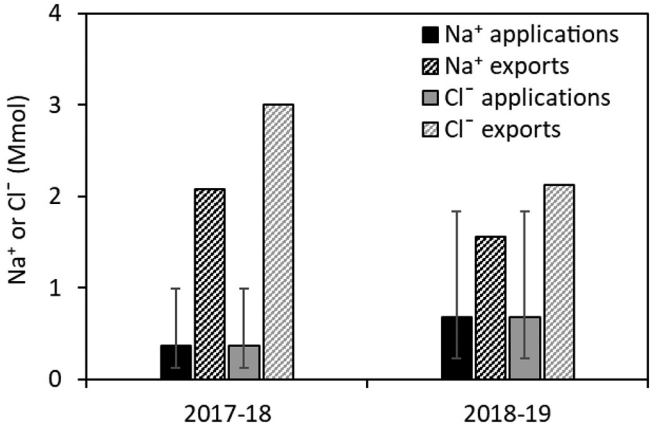

Fig. 10. Annual Na^+ (black) and Cl^- (gray) estimated applications (solid bars) and calculated exports (striped bars) for the karst spring. Thin black bars for the estimated application rates show the upper and lower boundaries when assuming salting outside of the Rockwoods Reservation occurred at double and half of the rate performed within the park, respectively. Note that data for fall 2019 were not available. Thus, the annual dataset for 2018–2019 is incomplete.

Despite the uncertainties related to estimating salt loads to the spring's recharge area, the higher Cl^- exports relative to Na^+ exports suggest greater retention of Na^+ in the system and more rapid delivery of Cl^- to groundwater. Together, our Na^+ and Cl^- load calculations indicate that delivery of salt ions to groundwater did not occur immediately and completely after road salt applications. While some salt was delivered rapidly via karst conduits (see groundwater salt peaks in Fig. 4), a significant amount of salt was also delivered through both conservative and non-conservative retention mechanisms that occurred within the soil and aquifer that caused delayed delivery of salt contamination to the spring outlet.

4. Conclusions

Our study provides evidence of mechanisms that cause road salt contaminant retention in vadose zone soils. The first mechanism, slow porewater movement, potentially delayed the arrival of both Na^+ and Cl^- to groundwater for 22–77 days once the salt reached the shallow soil. However, these calculations likely underestimate the delivery timing due to complex flow paths in the vadose zone and variable depths of the water table. The second mechanism, ion exchange reactions, caused retention for up to 5 months of deicer-derived Na^+ loads in the soil and gradual release months after salt applications had ceased. Cation exchanges with Na^+ ions also caused the release of base cations (e.g., Ca^{2+}, Mg^{2+}, and K^+) to porewaters. The loss of these cations can have detrimental effects on soil health and plant growth (Willmert et al., 2018). Cation exchange reactions triggered by road salt applications could also cause the mobilization of trace elements to porewaters (Nelson et al., 2009; Sun et al., 2015; Wu and Kim, 2017). These elements are typically important micronutrients at low concentrations, but, at higher concentrations, can cause toxicity issues.

We also found that exported annual Na^+ and Cl^- loads in groundwater exceeded estimated applications to the recharge area. Higher outputs compared with inputs of Na^+ and Cl^- may, in part, provide evidence of long-term accumulation of salt ions within the watershed, though we acknowledge that difficulties in obtaining accurate road salt application rate data may have led us to underestimate road salt inputs to the catchment. Nevertheless, at both seasonal and annual timescales, exported Na^+ loads were lower than Cl^- loads. We also found that seasonal Na^+ loads were more consistent across time compared to Cl^- loads. Loads of Cl^- were mainly affected by conservative retention mechanisms (e.g., slow soil porewater movement, diffuse flow through the aquifer), but Na^+ was affected by both conservative and non-conservative (e.g., cation exchange in soil) mechanisms. The relatively fast flushing of Cl^- from soils resulted in a rapid decrease of exchangeable Cl^- concentrations after road salt applications, while ESP in soils remained relatively high at least 5 months after the cessation of deicer applications. Thus, interactions between Na^+ and the vadose zone substrate delayed and decreased (by up to 30.8%) Na^+ transport across hydrologic reservoirs, leading to lower and more uniform delivery of Na^+ to groundwater over time.

Furthermore, our study illustrated how complex flow paths, especially in karst systems, led to both nearly immediate delivery of salts to the spring via conduits as well as slower release of salts to the spring from soils and diffusive flow over longer timescales. We found that peaks in soil porewater and karst groundwater Na^+ and Cl^- concentrations occurred simultaneously and shortly after individual salt applications. The concurrent increase in these ions in both soil waters and groundwaters following road deicing events suggests that there was rapid transmission of salt ions through conduits into the karst aquifer and hence no difference in the delivery timing of ion pulses to these hydrologic reservoirs. Without rapid transport mechanisms through the aquifer (i.e., conduits), a delayed peak in salt ions would be expected for the spring. The rapid conduit transmission of road salt contamination through the aquifer caused Cl^- concentrations in the spring to occasionally go above the USEPA chronic toxicity regulatory limit, which can harm aquatic ecosystems.

Our study provides evidence that soils are an important reservoir for road deicing salts before they reach deeper hydrological systems. The salt retention mechanisms identified here likely contributed to the long term increases in background salinity levels in freshwaters observed worldwide (Corsi et al., 2015; Hasenmueller and Robinson, 2016; Kaushal et al., 2018; Moore et al., 2020). We provide evidence of the important role of soils in the transport and retention of winter deicing salts to freshwater bodies. Thus, the interactions between soils and road salts need to be considered in the assessment of the environmental impacts of deicing agents on ecosystems and freshwater resources, as well as for the design of mitigation strategies for road salt contamination.

CRediT authorship contribution statement

Lead author Baraza oversaw field and lab work and performed the data analysis, and she and coauthor Hasenmueller were both involved in experimental design, data interpretation, and manuscript preparation. Both authors approve this article for submission.

Declaration of competing interest

The authors declare that they have no known competing financial interests or personal relationships that could have appeared to influence the work reported in this paper.

Acknowledgements

This work was funded by research grants awarded to TB from the Karst Waters Institute William L. and Diane C. Wilson Scholarship in Karst Science, The Geological Society of America Graduate Student Research Program, the Saint Louis University College of Arts & Sciences Graduate/Undergraduate Research Collaboration Fund, and other funds from Saint Louis University. The ICP-OES data for this study were collected with a PerkinElmer Optima 8300 instrument funded by the National Science Foundation (CHE-1626501) and Saint Louis University. We thank those who helped with field and laboratory work as well as MDC for providing access to the Rockwoods Reservation property and road salt application rates and dates for the roadways at the site. We appreciate thorough and thoughtful comments from Dr. Andrew Guswa and two anonymous reviewers, whose input helped improve the manuscript.

Appendix A. Supplementary data

Supplementary data, including detailed site and method descriptions, tables, and figures, that are mentioned in this paper are included in a separate file in this submission. Supplementary data for this article can be found online at https://doi.org/10.1016/j.scitotenv.2020.142240.

References

Amrhein, C., Strong, J.E., Mosher, P.A., 1992. Effect of deicing salts on metal and organic matter mobilization in roadside soils. Environ. Sci. Technol 26, 703–709. https://doi.org/10.2134/jeq1990.00472425001900040022x.

Asensio, E., Ferreira, V.J., Gil, G., García-Armingol, T., López-Sabirón, A.M., Ferreira, G., 2017. Accumulation of de-icing salt and leaching in Spanish soils surrounding roadways. Int. J. Environ. Res. Public Health 14. https://doi.org/10.3390/ijerph14121498.

Bäckström, M., Karlsson, S., Bäckman, L., Folkeson, L., Lind, B., 2004. Mobilisation of heavy metals by deicing salts in a roadside environment. Water Res. 38, 720–732. https://doi.org/10.1016/j.watres.2003.11.006.

Bastviken, D., Thomsen, F., Svensson, T., Karlsson, S., Sandén, P., Shaw, G., Matucha, M., Öberg, G., 2007. Chloride retention in forest soil by microbial uptake and by natural chlorination of organic matter. Geochim. Cosmochim. Acta 71, 3182–3192. https://doi.org/10.1016/j.gca.2007.04.028.

Bird, D.L., Groffman, P.M., Salice, C.J., Moore, J., 2018. Steady-state land cover but non-steady-state major ion chemistry in urban streams. Environ. Sci. Technol. 52, 13015–13026. https://doi.org/10.1021/acs.est.8b03587.

Clements, W.H., Kotalik, C., 2016. Effects of major ions on natural benthic communities: an experimental assessment of the US Environmental Protection Agency aquatic life benchmark for conductivity. Freshw. Sci. 35, 126–138. https://doi.org/10.1086/685085.

Corsi, S.R., Graczyk, D.J., Geis, S.W., Booth, N.L., Richards, K.D., 2010. A fresh look at road salt: aquatic toxicity and water-quality impacts on local, regional, and national scales. Environ. Sci. Technol. 44, 7376–7382. https://doi.org/10.1021/es101333u.

Corsi, S.R., De Cicco, L.A., Lutz, M.A., Hirsch, R.M., 2015. River chloride trends in snow-affected urban watersheds: increasing concentrations outpace urban growth rate and are common among all seasons. Sci. Total Environ. 508, 488–497. https://doi.org/10.1016/j.scitotenv.2014.12.012.

Criss, R.E., 1999. Principles of stable isotope distribution. Oxford University Press, New York.

Criss, R.E., 2010. A darcian model for the flow of big spring and the hydraulic head in the Ozark aquifer, Missouri, USA. Acta Carsologica 39, 379–387. https://doi.org/10.3986/ac.v39i2.106.

Criss, R.E., Winston, W.E., 2008. Discharge predictions of a rainfall-driven theoretical hydrograph compared to common models and observed data. Water Resour. Res. 44, 1–9. https://doi.org/10.1029/2007WR006415.
Criss, R.E., Davisson, L., Surbeck, H., Winston, W.E., 2007. Isotopic methods. Methods in Karst Hydrogeology. Taylor & Francis, London, UK, pp. 123–145.
Dugan, H.A., Bartlett, S.L., Burke, S.M., Doubek, J.P., Krivak-Tetley, F.E., Skaff, N.K., Summers, J.C., Farrell, K.J., McCullough, I.M., Morales-Williams, A.M., Roberts, D.C., Ouyang, Z., Scordo, F., Hanson, P.C., Weathers, K.C., 2017. Salting our freshwater lakes. Proc. Natl. Acad. Sci. 114, 4453–4458. https://doi.org/10.1073/pnas.1620211114.
Fay, L., Shi, X., 2012. Environmental impacts of chemicals for snow and ice control: state of the knowledge. Water Air Soil Pollut. 223, 2751–2770. https://doi.org/10.1007/s11270-011-1064-6.
Foos, A., 2003. Spatial distribution of road salt contamination of natural springs and seeps, Cuyahoga Falls, Ohio, USA. Environ. Geol. 44, 14–19. https://doi.org/10.1007/s00254-002-0724-7.
Frederickson, G.C., Criss, R.E., 1999. Isotope hydrology and residence times of the unimpounded Meramec River Basin, Missouri. Chem. Geol. 157, 303–317. https://doi.org/10.1016/S0009-2541(99)00008-X.
Godwin, K.S., Hafner, S.D., Buff, M.F., 2003. Long-term trends in sodium and chloride in the Mohawk River, New York: the effect of fifty years of road-salt application. Environ. Pollut. 124, 273–281. https://doi.org/10.1016/S0269-7491(02)00481-5.
Green, S.M., Machin, R., Cresser, M.S., 2008. Effect of long-term changes in soil chemistry induced by road salt applications on N-transformations in roadside soils. Environ. Pollut. 152, 20–31. https://doi.org/10.1016/j.envpol.2007.06.005.
Haake, D.M., Knouft, J.H., 2019. Comparison of contributions to chloride in urban stormwater from winter brine and rock salt application. Environ. Sci. Technol. 53, 11888–11895. https://doi.org/10.1021/acs.est.9b02864.
Harrison, R.W., 1997. Bedrock geologic map of the St. Louis 30′ × 60′ Quadrangle, Missouri and Illinois: U.S. Geological Survey Miscellaneous Investigation Series Map I-2533, scale 1:100,000.
Harte, P.T., Trowbridge, P.R., 2010. Mapping of road-salt-contaminated groundwater discharge and estimation of chloride load to a small stream in southern New Hampshire, USA. Hydrol. Process. 24, 2349–2368. https://doi.org/10.1002/hyp.7645.
Hasenmueller, E., 2011. The Hydrology and Geochemistry of Urban and Rural Watersheds in East-Centry Missouri. p. 382.
Hasenmueller, E.A., Criss, R.E., 2013. Geochemical techniques to discover open cave passage in karst spring systems. Appl. Geochem. 29, 126–134. https://doi.org/10.1016/j.apgeochem.2012.11.004.
Hasenmueller, E.A., Robinson, H.K., 2016. Hyporheic zone flow disruption from channel linings: implications for the hydrology and geochemistry of an urban stream, St. Louis, Missouri, USA. J. Earth Sci. 27, 98–109. https://doi.org/10.1007/s12583-016-0632-5.
Howard, K.W.F., Haynes, J., 1993. Contamination due to road de-icing chemicals - salt balance implications. Geosci. Canada 20, 1–8.
Kaushal, S.S., Likens, G.E., Pace, M.L., Utz, R.M., Haq, S., Gorman, J., Grese, M., 2018. Freshwater salinization syndrome on a continental scale. Proc. Natl. Acad. Sci. 115, E574–E583. https://doi.org/10.1073/pnas.1711234115.
Kelly, V.R., Lovett, G.M., Weathers, K.C., Findlay, S.E.G., Strayer, D.L., Burns, D.J., Likens, G.E., 2008. Long-term sodium chloride retention in a rural watershed: legacy effects of road salt on streamwater concentration. Environ. Sci. Technol. 42, 410–415. https://doi.org/10.1021/es071391l.
Kincaid, D.W., Findlay, S.E.G., 2009. Sources of elevated chloride in local streams: groundwater and soils as potential reservoirs. Water Air Soil Pollut. 203, 335–342. https://doi.org/10.1007/s11270-009-0016-x.
Lancaster, N.A., Bushey, J.T., Tobias, C.R., Song, B., Vadas, T.M., 2016. Impact of chloride on denitrification potential in roadside wetlands. Environ. Pollut. 212, 216–223. https://doi.org/10.1016/j.envpol.2016.01.068.
Meriano, M., Eyles, N., Howard, K.W.F., 2009. Hydrogeological impacts of road salt from Canada's busiest highway on a Lake Ontario watershed (Frenchman's Bay) and lagoon, City of Pickering. J. Contam. Hydrol. 107, 66–81. https://doi.org/10.1016/j.jconhyd.2009.04.002.
Moore, J., Bird, D.L., Dobbis, S.K., Woodward, G., 2017. Nonpoint source contributions drive elevated major ion and dissolved inorganic carbon concentrations in urban watersheds. Environ. Sci. Technol. Lett. 4, 198–204. https://doi.org/10.1021/acs.estlett.7b00096.
Moore, J., Fanelli, R.M., Sekellick, A.J., 2020. High-frequency data reveal deicing salts drive elevated specific conductance and chloride along with pervasive and frequent exceedances of the U.S. Environmental Protection Agency aquatic life criteria for chloride in urban streams. Environ. Sci. Technol. 54, 778–789. https://doi.org/10.1021/acs.est.9b04316.
Mueller, M.H., Alaoui, A., Kuells, C., Leistert, H., Meusburger, K., Stumpp, C., Weiler, M., Alewell, C., 2014. Tracking water pathways in steep hillslopes by δ18O depth profiles of soil water. J. Hydrol. 519, 340–352. https://doi.org/10.1016/j.jhydrol.2014.07.031.
National Atmospheric Deposition Program (NADP), 2020. Precipitation-Weighed Mean (PWM) Concentrations. National Trends Network http://nadp.slh.wisc.edu/data.
National Oceanic and Atmospheric Administration (NOAA), 2019. Local climatological dataset. URL. https://www.ncdc.noaa.gov/cdo-web/.
Nelson, S.S., Yonge, D.R., Barber, M.E., 2009. Effects of road salts on heavy metal mobility in two eastern Washington soils. J. Environ. Eng. 135, 505–510. https://doi.org/10.1061/(asce)0733-9372(2009)135:7(505).
Norrström, A.C., Jacks, G., 1998. Concentration and fractionation of heavy metals in roadside soils receiving de-icing salts. Sci. Total Environ. 218, 161–174. https://doi.org/10.1016/S0048-9697(98)00203-4.
Novotny, E.V., Murphy, D., Stefan, H.G., 2008. Increase of urban lake salinity by road deicing salt. Sci. Total Environ. 406, 131–144. https://doi.org/10.1016/j.scitotenv.2008.07.037.
Ostendorf, D.W., Peeling, D.C., Mitchell, T.J., Pollock, S.J., 2001. Chloride persistence in a deiced access road drainage system. J. Environ. Qual. 30, 1756. https://doi.org/10.2134/jeq2001.3051756x.
Perera, N., Gharabaghi, B., Howard, K., 2013. Groundwater chloride response in the Highland Creek watershed due to road salt application: a re-assessment after 20 years. J. Hydrol. 479, 159–168. https://doi.org/10.1016/j.jhydrol.2012.11.057.
Potapova, M., Charles, D.F., 2003. Distribution of benthic diatoms in U.S. rivers in relation to conductivity and ionic composition. Freshw. Biol. 48, 1311–1328. https://doi.org/10.1046/j.1365-2427.2003.01080.x.
Rhodes, A.L., Guswa, A.J., 2016. Storage and release of road-salt contamination from a calcareous lake-basin fen, western Massachusetts, USA. Sci. Total Environ. 545–546, 525–545. https://doi.org/10.1016/j.scitotenv.2015.12.060.
Robinson, H.K., Hasenmueller, E.A., 2017. Transport of road salt contamination in karst aquifers and soils over multiple timescales. Sci. Total Environ. 603–604, 94–108. https://doi.org/10.1016/j.scitotenv.2017.05.244.
Robinson, H.K., Hasenmueller, E.A., Chambers, L.G., 2017. Soil as a reservoir for road salt retention leading to its gradual release to groundwater. Appl. Geochem. 83, 72–85. https://doi.org/10.1016/j.apgeochem.2017.01.018.
Rossi, R.J., Bain, D.J., Elliott, E.M., Divers, M., O'Neill, B., 2017. Hillslope soil water flowpaths and the dynamics of roadside soil cation pools influenced by road deicers. Hydrol. Process. 31, 177–190. https://doi.org/10.1002/hyp.10989.
Sassan, D., Kahl, S., 2007. Salt Loading Due to Private Winter Maintenance Practices. Plymouth State University Center for the Environment https://www.des.nh.gov/organization/divisions/water/wmb/was/salt-reduction-initiative/so-i93-impaired/documents/salt-loading-final-report.pdf.
Scott, R., Goulden, T., Letman, M., Hayward, J., Jamieson, R., 2019. Long-term evaluation of the impact of urbanization on chloride levels in lakes in a temperate region. J. Environ. Manag. 244, 285–293. https://doi.org/10.1016/j.jenvman.2019.05.029.
Shaughnessy, A.R., Prener, C.G., Hasenmueller, E.A., 2019. An R package for correcting continuous water quality monitoring data for drift. Environ. Monit. Assess. 191, 445. https://doi.org/10.1007/s10661-019-7586-x.
Shourd, M.L., Levin, H.L., 1976. Chondrites in the upper Plattin Subgroup (middle Ordovician) of eastern Missouri. J. Paleontol. 50, 260–268.
Snodgrass, J.W., Moore, J., Lev, S.M., Casey, R.E., Ownby, D.R., Flora, R.F., Izzo, G., 2017. Influence of modern stormwater management practices on transport of road salt to surface waters. Environ. Sci. Technol. 51, 4165–4172. https://doi.org/10.1021/acs.est.6b03107.
Stets, E.G., Lee, C.J., Lytle, D.A., Schock, M.R., 2018. Increasing chloride in rivers of the conterminous U.S. and linkages to potential corrosivity and lead action level exceedances in drinking water. Sci. Total Environ. 613–614, 1498–1509. https://doi.org/10.1016/j.scitotenv.2017.07.119.
Sun, H., Alexander, J., Gove, B., Koch, M., 2015. Mobilization of arsenic, lead, and mercury under conditions of sea water intrusion and road deicing salt application. J. Contam. Hydrol. 180, 12–24. https://doi.org/10.1016/j.jconhyd.2015.07.002.
Thomas, E.M., Lin, H., Duffy, C.J., Sullivan, P.L., Holmes, G.H., Brantley, S.L., Jin, L., 2013. Spatiotemporal patterns of water stable isotope compositions at the shale hills critical zone observatory: linkages to subsurface hydrologic processes. Vadose Zo. J. 12, 0. https://doi.org/10.2136/vzj2013.01.0029.
Thunqvist, E.L., 2004. Regional increase of mean chloride concentration in water due to the application of deicing salt. Sci. Total Environ. 325, 29–37. https://doi.org/10.1016/j.scitotenv.2003.11.020.
U.S. Department of Agriculture, 2020. Soil Survey Geographic Database. NRCS Web Soil Survey.
U.S. Environmental Protection Agency (USEPA), 1988. Ambient Water Quality for Criteria for Chloride.
Vitale, S.A., Robbins, G.A., McNaboe, L.A., 2017. Impacts of road salting on water quality in fractured crystalline bedrock. J. Environ. Qual. 46, 288. https://doi.org/10.2134/jeq2016.10.0411.
Wilhelm, J.F., Bain, D.J., Green, M.B., Bush, K.F., McDowell, W.H., 2019. Trace metals in Northern New England streams: evaluating the role of road salt across broad spatial scales with synoptic snapshots. PLoS One 14, 1–20. https://doi.org/10.1371/journal.pone.0212011.
Willmert, H.M., Osso, J.D., Twiss, M.R., Langen, T.A., 2018. Winter road management effects on roadside soil and vegetation along a mountain pass in the Adirondack Park, New York, USA. J. Environ. Manag. 225, 215–223. https://doi.org/10.1016/j.jenvman.2018.07.085.
Wu, J., Kim, H., 2017. Impacts of road salts on leaching behavior of lead contaminated soil. J. Hazard. Mater. 324, 291–297. https://doi.org/10.1016/j.jhazmat.2016.10.059.